

Supplementary Information

Thermoelectric properties and thermal stability of layered chalcogenides, TlScQ₂, Q= Se, Te

Vijayakumar Sajitha Aswathy[§], Cheriyaedath Raj Sankar^{§*}, Manoj Raama Varma[§], Abdeljalil Assoud[†], Mario Bieringer[‡], and Holger Kleinke^{†#}

[§]Materials Science and Technology Division and Academy of Scientific and Innovative Research (AcSIR), CSIR-National Institute for Interdisciplinary Science and Technology, Thiruvananthapuram-695019, Kerala, India

[‡]Department of Chemistry and Manitoba Institute for Materials, University of Manitoba, Winnipeg, Manitoba R3T 2N2, Canada

[†]Department of Chemistry and [#]Waterloo Institute for Nanotechnology, University of Waterloo, Waterloo, ON N2L 3G1, Canada

*Email: rajsankar@niist.res.in

Supporting Information

Crystal structure refinement data for two different 'TlScTe₂' crystals:

Table S1: Crystallographic information of Tl_{0.96}ScTe₂

Empirical formula	Tl _{0.964(4)} ScTe ₂
Formula weight	497.18 g/mol
Temperature	298(2) K
Wavelength	0.71073 Å
Crystal system	Rhombohedral
Space group	<i>R</i> Error! <i>m</i>
<i>A</i>	4.2133(2) Å
<i>C</i>	24.088(2) Å
Volume	370.32(4) Å ³
<i>Z</i>	3

Density (calculated)	6.688 g/cm ³
Absorption coefficient	44.18 mm ⁻¹
F(000)	609
Crystal size	0.04 x 0.04 x 0.02 mm
Reflections collected	1303
Independent reflections [R(int)]	246 [0.0377]
Completeness to $\theta = 34.97^\circ$	99.6 %
Refinement method	Full-matrix least-squares on F ²
Data \ restraints \ parameters	246 \ 0 \ 10
Goodness-of-fit on F ²	1.187
R indices (all data)	R1 = 0.0306, wR2 = 0.0826
Extinction coefficient	0.0058(7)
Largest diff. peak and hole	3.97 and -2.39 e/Å ³

$$R = \frac{\sum ||F_o| - |F_c||}{\sum |F_o|}, \quad wR = \left\{ \frac{\sum [w(|F_o|^2 - |F_c|^2)^2]}{\sum [w(|F_o|^4)]} \right\}^{1/2} \text{ and calc}$$

$$w = 1 / [\sigma^2(F_o^2) + (0.0171P)^2 + 0.0000P] \text{ where } P = (F_o^2 + 2F_c^2) / 3$$

Table S2: Atomic coordinates and displacement parameters of $\text{Tl}_{0.96}\text{ScTe}_2$.

Atom	Site	Z	Occupancy	$U_{11}/\text{\AA}^2$	$U_{33}/\text{\AA}^2$	$U_{12}/\text{\AA}^2$	$U_{\text{eq}}/\text{\AA}^2$
Tl	$3a$	0	0.964(4)	0.0253(3)	0.0220(4)	0.0127(2)	0.0242(3)
Sc	$3b$	0.5	1	0.0116(6)	0.014(1)	0.0058(3)	0.0131(4)
Te	$6c$	0.23477(2)	1	0.0116(3)	0.0120(4)	0.0058(2)	0.0120(2)

For all atoms $x = y = 0$; $U_{11} = U_{22}$; $U_{23} = U_{13} = 0$.
 U_{eq} is defined as one third of the trace of the orthogonalized U_{ij} tensor.

Table S3: Crystallographic information of $\text{Tl}_{0.975}\text{ScTe}_2$

Empirical formula	$\text{Tl}_{0.975(3)}\text{ScTe}_2$
Formula weight	499.43 g/mol
Temperature	298(2) K
Wavelength	0.71073 Å
Crystal system	Rhombohedral
Space group	<i>R</i> 3m
A	4.2173(6) Å
C	24.112(3) Å
Volume	371.39(9) Å ³
Z	3
Density (calculated)	6.768 g/cm ³
Absorption coefficient	45.219 mm ⁻¹
F(000)	618
Crystal size	0.04 x 0.04 x 0.02 mm
Reflections collected	949
Independent reflections [R(int)]	171 [0.0229]
Completeness to $\theta = 30.04^\circ$	99.6 %
Refinement method	Full-matrix least-squares on F ²
Data \ restraints \ parameters	171 \ 0 \ 10
Goodness-of-fit on F ²	1.060
R indices (all data)	R1 = 0.0123, wR2 = 0.0285
Extinction coefficient	0.000996(7)
Largest diff. peak and hole	0.551 and -1.011 e/Å ³

$$R = \frac{\sum ||F_o| - |F_c||}{\sum |F_o|}, wR = \left\{ \frac{\sum [w(|F_o|^2 - |F_c|^2)^2]}{\sum [w(|F_o|^4)]} \right\}^{1/2} \text{ and calc}$$

$$w = 1 / [\sigma^2(F_o^2) + (0.0171P)^2 + 0.0000P] \text{ where } P = (F_o^2 + 2F_c^2) / 3$$

Table S4: Atomic coordinates and displacement parameters of $\text{Tl}_{0.975}\text{ScTe}_2$.

Atom	Site	Z	<i>Occupancy</i>	$U_{11}/\text{\AA}^2$	$U_{33}/\text{\AA}^2$	$U_{12}/\text{\AA}^2$	$U_{\text{eq}}/\text{\AA}^2$
Tl	$3a$	0	0.9753(3)	0.02704(3)	0.02156(4)	0.01352(1)	0.02521(2)
Sc	$3b$	0.5	1	0.01335(9)	0.0121(2)	0.00668(5)	0.01295(8)
Te	$6c$	0.234722(4)	1	0.01260(2)	0.01191(4)	0.00630(1)	0.01237(2)

For all atoms $x = y = 0$; $U_{11} = U_{22}$; $U_{23} = U_{13} = 0$.
 U_{eq} is defined as one third of the trace of the orthogonalized U_{ij} tensor.

Band structure calculations

Table S5: k-path designation for band dispersion of TlScTe₂

Label	$x k_1, x k_2, x k_3$
G (or Γ)	0, 0, 0
L	0.5, 0, 0
B	0.8189, 0.5, 0.1811
Z	0.5, 0.5, 0.5
G	0, 0, 0
X	0.3405, 0, 0.3405
F	0.5, 0.5, 0
P1	0.6595, 0.6595, 0.1811
Z	0.5, 0.5, 0.5
P	0.8189, 0.3405, 0.3405

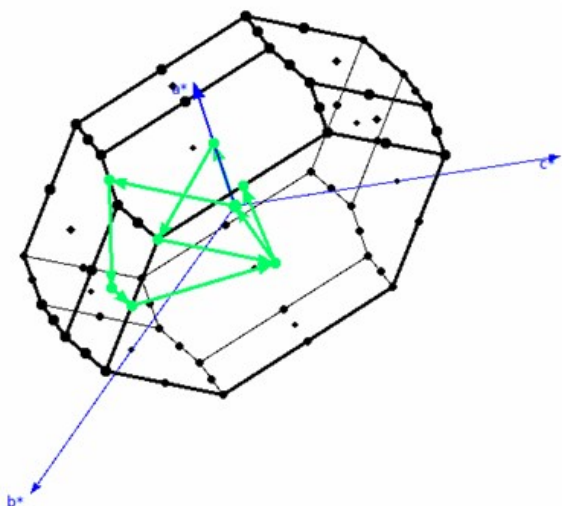


Figure S1: Brillouin zone described for the rhombohedral TlScTe₂

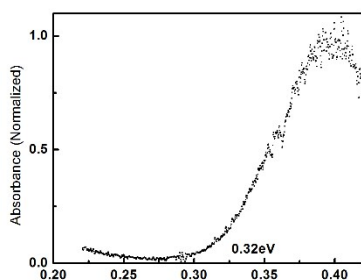
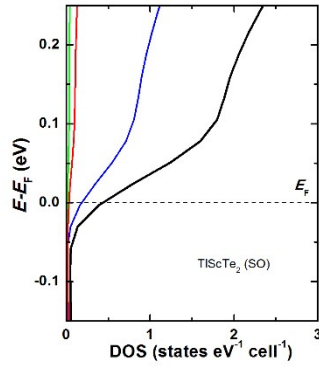


Figure S2: Infra red absorption edge of the semi conductor, TlScSe₂ measured by using IR diffused reflectance spectroscopy, followed by Kubelka Munk transformation. The absorption edge is identified as 0.32 eV.



Expanded region of the figure 2(d) in the main text to show the Fermi level

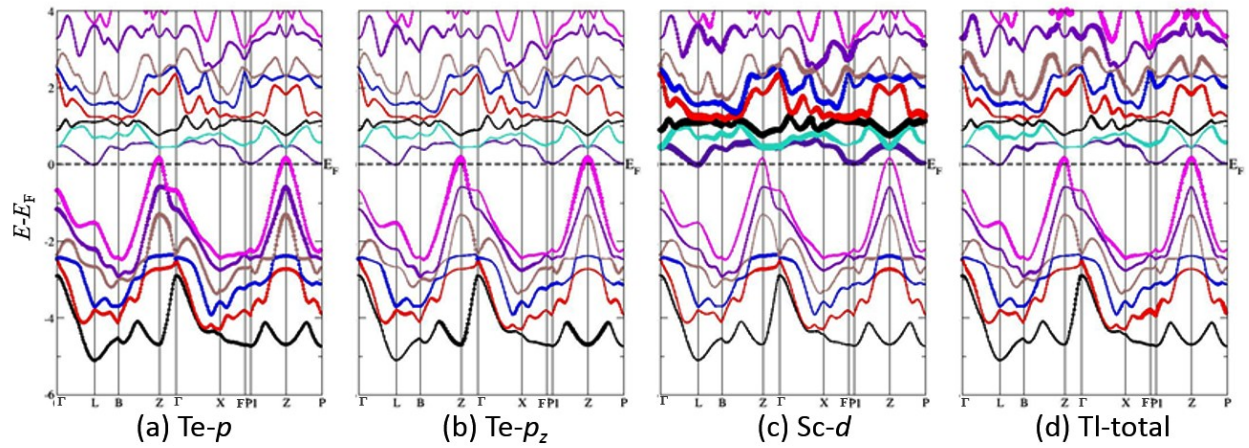


Figure S3: Band structures calculated for TlScTe₂ with fat band representation for individual elements/orbitals as labelled. The horizontal dashed line represents E_F . Different colors are used to represent the individual bands.

More evidences supporting the thermal instability of TlScQ₂

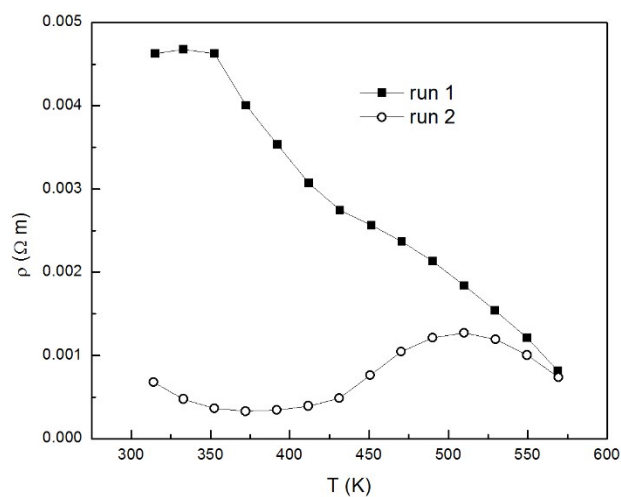


Figure S4: Resistivity vs Temperature data obtained for a back to back measurement on the same TlScSe_2 sample

The thermogravimetric data (Figure S5) for TlScSe_2 shows significant loss of weight upon heating above room temperature. There is no apparent weight loss for TlScTe_2 during warming in the temperature range specified on the figure.

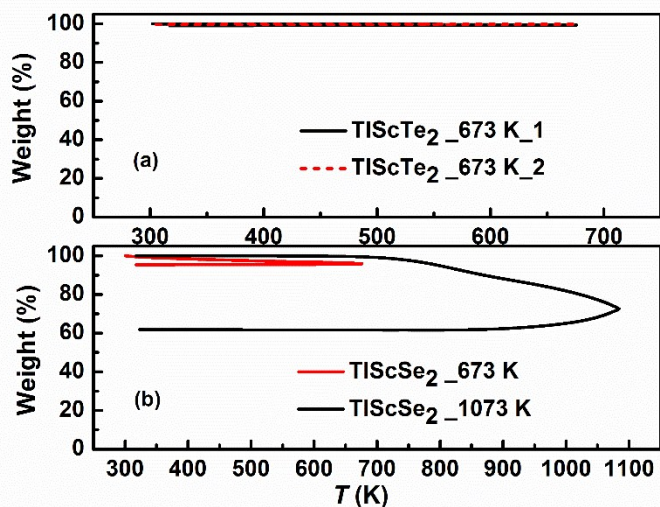


Figure S5: TG of (a) TlScTe_2 and (b) TlScSe_2 upon two consecutive cycles.

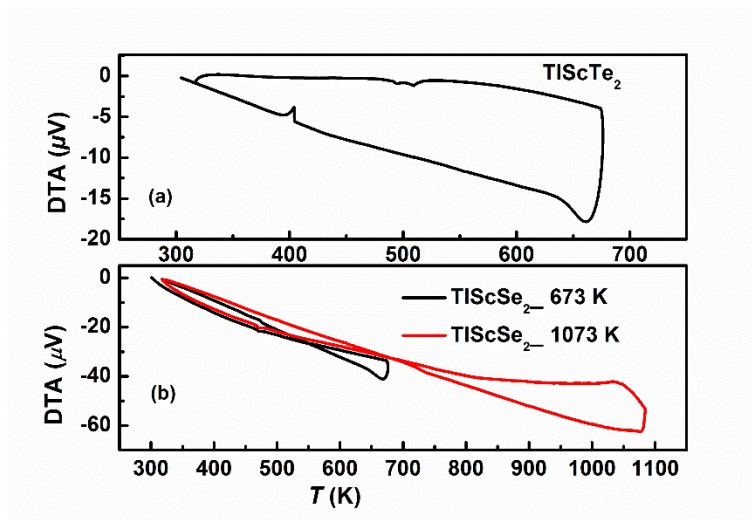


Figure S6: DTA of (a) TlScTe₂ and (b) TlScSe₂

Differential thermal analyses of the samples are as shown in figure S6. The endothermic dip is observed for TlScTe₂ at around 510 K corresponding to the melting point of Tl₂Te₃. No transitions were observed in DTA of TlScSe₂.

TlScSe₂ undergoes massive weight loss while heating up to 800 °C, confirming sample decomposition. This is evident from the 'ZEM-3' measurements as well. The powder XRD patterns, before and after the measurement are shown in figure S7.

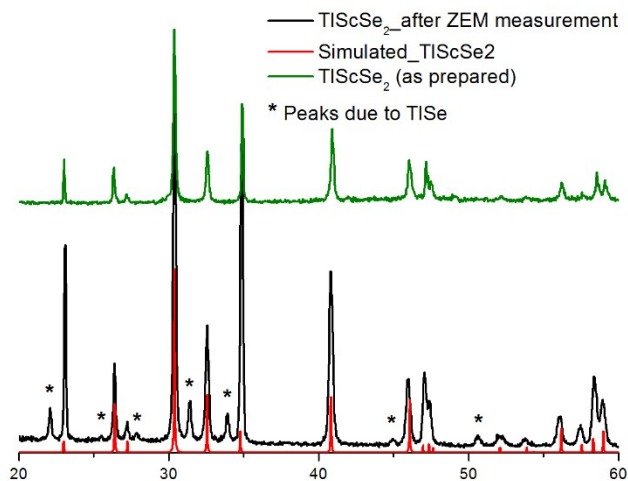


Figure S7: Powder XRD pattern of the ZEM pellet (black line) of TlScSe₂ after the high temperature physical property measurement and that of the as prepared sample (green line). TlSe is found to be one of the solid phases (marked peaks) remained after the decomposition. Red line represents the simulated PXRD pattern of TlScSe₂. The difference of intensities may be due to the preferential orientation (usually observed in layered compounds).

TlScSe₂ is unstable when warmed up above room temperature, which was reflected in our back to back measurement of electrical resistivity, ρ as shown in figure S4. However, back to back ρ -T measurements on TlScTe₂ sample, were found to be more or less reproducible as shown below.

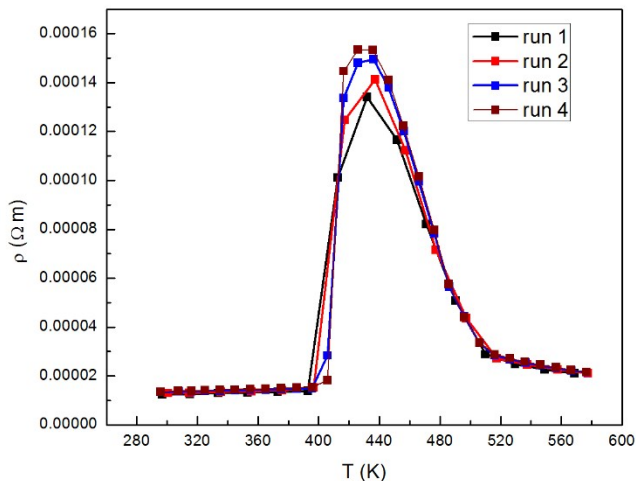


Figure S8: Resistivity vs Temperature plots obtained for back to back measurements of the same TlScTe₂ sample.

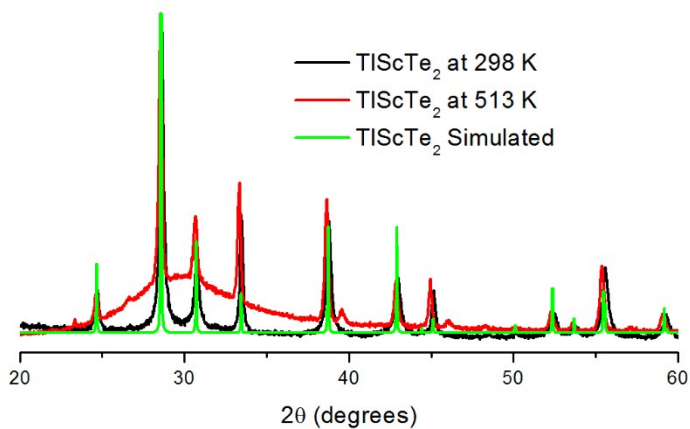


Figure S9: Comparison of PXRD patterns of (a) the pristine sample at room temperature (black line), (b) when warmed up to 513 K (red line) along with (c) the simulated pattern for TlScTe₂. The secondary phase formed melts and only the solid remained (TlScTe₂) is observable here.

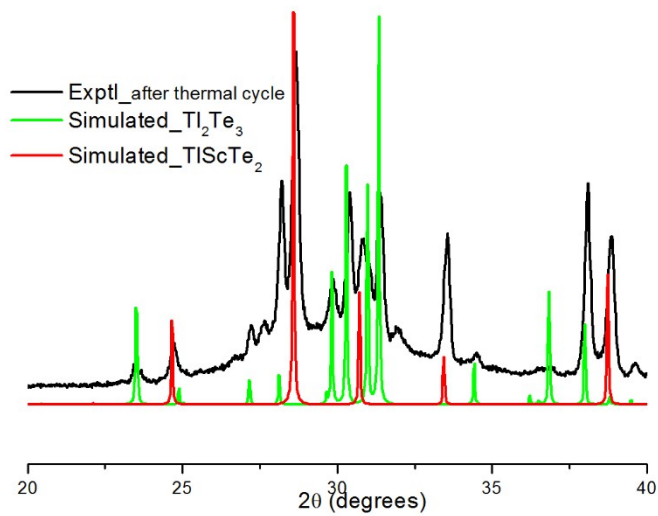


Figure S10: Powder XRD pattern obtained at 298 K, after the HT-XRD thermal cycling. A secondary phase identified in the remaining sample is Tl_2Te_3 (along with $TlScTe_2$).

SEM-EDX results

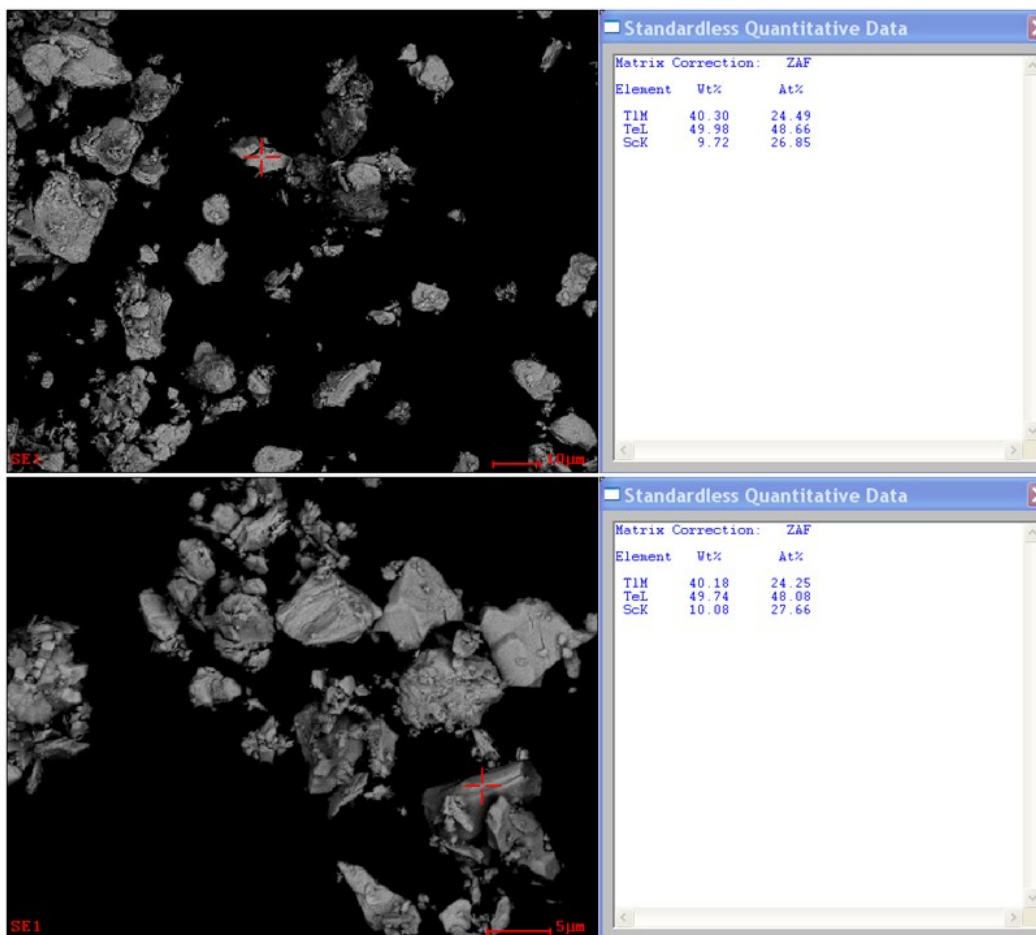


Figure S11: Two representative SEM picture and EDX results for pristine sample of TlScTe₂.

Table S6: EDX results obtained from 10 different spots from the pristine sample

Pristine	1	2	3	4	5	6	7	8	9	10	Theoretical
Tl	23.60	24.24	24.25	24.70	24.54	23.49	24.10	23.84	24.49	24.29	25
Te	47.85	48.48	48.08	47.28	47.66	48.18	47.88	48.04	48.66	47.60	50
Sc	28.55	27.28	27.66	28.02	27.80	28.33	28.02	28.11	26.85	28.11	25

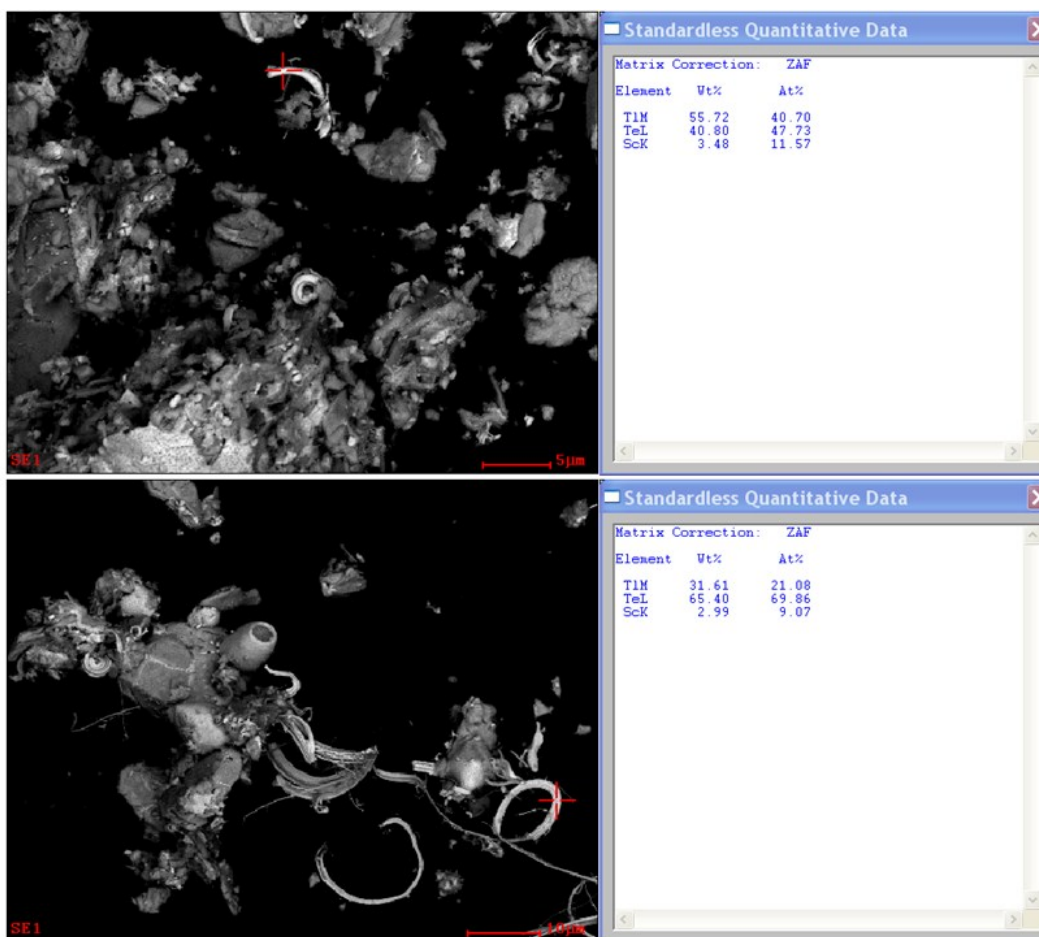


Figure S12: Two representative SEM pictures and EDX results of HT-XRD sample of TlScTe_2 . The microstructure is nonuniform and elemental ratio is significantly different from spot to spot as opposed to that in the pristine sample.

Table S7: EDX results obtained from 12 different spots from the HT-XRD sample

HT-XRD	1	2	3	4	5	6	7	8	9	10	11	12
Tl	14.21	40.70	16.58	16.73	13.11	24.44	17.94	18.29	34.28	28.76	21.08	14.30
Te	30.72	47.73	32.51	30.81	30.38	56.73	39.47	46.70	54.13	63.97	69.86	30.05
Sc	55.02	11.57	50.92	52.46	56.51	18.83	42.60	35.01	11.59	7.27	9.07	55.65